ELSEVIER

Atmospheric Research 81 (2006) 176–185

ATMOSPHERIC RESEARCH

www.elsevier.com/locate/atmos

Atmospheric aerosol load as derived from space

Alexander A. Kokhanovsky *, Wolfgang von Hoyningen-Huene, John P. Burrows

Institute of Environmental Physics, Bremen University, Otto Hahn Allee 1, D-28213 Bremen, Germany

Received 5 February 2005; accepted 20 December 2005

Abstract

The paper is devoted to the introduction of a new technique to derive the aerosol mass load and particle number concentration from spaceborne observations. It is based on the simultaneous determination of the spectral aerosol optical thickness (AOT) τ and the spectral effective Lambertian ground reflectance A for a given scene using the aerosol retrieval algorithm developed by us. The aerosol mass is proportional to the measured AOT with the coefficient of proportionality dependent on the effective radius a_{ef} of aerosol particles. The value of a_{ef} can be estimated from the slope of the function $\tau(\lambda)$, where λ is the wavelength. The developed technique is applied to SeaWiFs imagery data over Moscow.

Keywords: Atmospheric aerosol; Pollution; Mie theory; Spaceborne remote sensing

1. Introduction

Remote sensing of aerosols from space involves several a priori assumptions. They are mostly related to the treatment of the ground reflection (surface spectra) and the shape of particles. Most of modern retrieval procedures assume the spherical shape of particles. This can lead to large biases in the retrieved aerosol optical thickness. For instance, it is known that the reflection function $R(\tau)$ of thin aerosol layers is directly proportional to the product $\tau p(\theta)$, where τ is the optical thickness, and $p(\theta)$ is the aerosol phase function. Wrong assumptions on the shape of particles can bias the phase function and, therefore, also the retrieved value of $\tau \sim R(\tau)/p(\theta)$. Von Hoyningen-Huene et al. (2003) have proposed an aerosol retrieval algorithm BAER, which is based not only on the conventional Look-Up-Table (LUT) approach for spheres but has a flexibility to deal with phase

* Tel.: +49 421218 2915; fax: +49 421218 4555.
E-mail address: alexk@iup.physik.uni-bremen.de (A.A. Kokhanovsky).

0169-8095/$ - see front matter © 2006 Elsevier B.V. All rights reserved.
doi:10.1016/j.atmosres.2005.12.001

functions of nonspherical particles and in particular with experimental phase functions of atmospheric aerosol. This improves the accuracy of the retrieval if the degree of nonsphericity of particles is known in advance or can be assessed by independent measurements. The retrievals of aerosol optical thickness using BAER closely follow the results obtained from ground-based sunphotometers (von Hoyningen-Huene et al., 2003; Kokhanovsky et al., 2004).

However, a problem arises, if one uses the experimental phase function. Namely, for the standard LUT approach, both the effective radius of particles $a_{ef}=3\langle V\rangle/\langle S\rangle$ ($\langle V\rangle$ is the average volume of particles, $\langle S\rangle$ is the average surface area of particles) and their columnar concentration $n=NL$ (N is the number of particles in a unit volume and L is the boundary layer height) can be directly retrieved fitting measured spectra to those stored in LUTs for various aerosol models (Tanre et al., 1999). This is not the case for algorithms based on the experimental phase functions. Then an additional procedure to retrieve a_{ef} and n from the spectral aerosol optical thickness is needed. Such procedures are widely available and can be posed as solutions of a certain class of inverse problems based on spectral extinction measurements (Yamamoto and Tanaka, 1969; King et al., 1978). However, operational satellite retrieval algorithms have quite considerable constraints with respect to the speed of calculations. So this path can not be followed.

With this in mind, we propose here a number of simple parameterizations. These parameterizations allow us to derive a_{ef} and n if the aerosol optical thickness spectrum is known. The results of the work are of importance for the improvement of the air quality forecasts using spaceborne observations (Al-Saadi et al., 2005). However, it must be emphasized that it is almost impossible to provide ground truth using surface observations to verify the results obtained from the satellite measurements in the qualitative way. Indeed, satellite measurements refer to the total atmospheric column and not to the point measurements (e.g., at 2 m height) as performed by particulate matter monitoring stations. However, the derived total atmospheric column aerosol optical thickness highly correlates with the ground particulate matter measurements as demonstrated, e.g., by Al-Saadi et al. (2005). Such correlations, if properly studied, can be used for the pollution monitoring from space (Griggs, 1975, 1979; Fraser, 1976; Fraser et al., 1984; Kaufman and Fraser, 1990; Gasso and Hegg, 1997, 2003).

2. Parameterizations

Neglecting the vertical variability of the aerosol extinction coefficient, we can represent the aerosol optical thickness at a given wavelength λ using the following equation:

$$\tau(\lambda) = n\langle C_{ext}(\lambda)\rangle \tag{1}$$

where

$$\langle C_{ext}(\lambda)\rangle = \langle s\rangle\langle Q_{ext}(\lambda)\rangle \tag{2}$$

is the average extinction cross section, $\langle s\rangle$ is the average geometrical cross section of particles and

$$\langle Q_{ext}(\lambda)\rangle = \langle C_{ext}(\lambda)\rangle/\langle s\rangle \tag{3}$$

is the average extinction efficiency factor. Let as assume that aerosol particles have a spherical shape. Then we have:

$$\langle s\rangle = \int_0^\infty \pi a^2 f(a)\mathrm{d}a \tag{4}$$

and

$$\langle Q_{\rm ext}(\lambda)\rangle = \frac{1}{\langle s\rangle}\int_0^\infty \pi a^2 Q_{\rm ext}(\lambda) f(a)\mathrm{d}a \tag{5}$$

by definition. Here $f(a)$ is the particle size distribution (PSD) and a is the radius of particles. We will assume that this function is given by the following expression:

$$f(a) = \frac{1}{a\sigma\sqrt{2\pi}}\exp\left\{-0.5\sigma^{-2}\ln^2\left[\frac{a}{a_{\rm m}}\right]\right\}, \tag{6}$$

where $a_{\rm m}$, σ are free parameters defining the effective radius $a_{\rm ef}=a_{\rm m}\exp(-2.5\sigma^2)$. The parameter σ is determined by the coefficient of variance Δ (the ratio of the standard deviation of the PSD to the mean radius) as $\sigma=\sqrt{\ln\left(1+\Delta^2\right)}$. Also it follows for the value of $\langle s\rangle$:

$$\langle s\rangle = \pi a_{\rm ef}^2\exp\left(-3\sigma^2\right). \tag{7}$$

The function $\langle Q_{\rm ext}(\lambda)\rangle$ can be found from Mie theory. In particular, we show the dependence of $\langle Q_{\rm ext}\rangle$ on the size parameter $x=2\pi a_{\rm ef}/\lambda$ in Fig. 1. Calculations were performed for the refractive indices of aerosol particles equal to 1.45+0.005i and 1.53+0.008i, which cover most of possible range of the variation of the aerosol refractive index in visible. Also we assumed that the coefficient of variance of the PSD $\Delta=1$. This means that the standard deviation of the PSD is equal to the average radius, which is often the case for the aerosol PSDs. Note that we have:

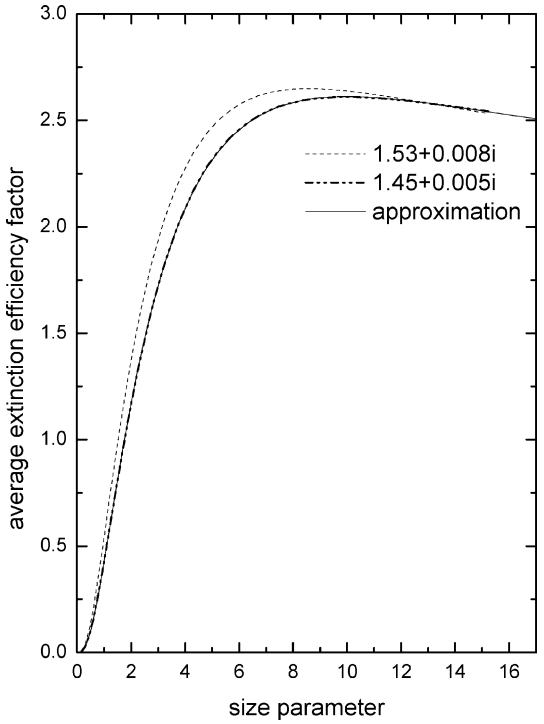

Fig. 1. Dependence of the average extinction efficiency factor on the effective size parameter $x=2\pi a_{\rm ef}/\lambda$ calculated using Mie theory as indicated in the text.

$\sigma \approx 0.8326$ in this case. It follows from Fig. 1 that both curves do not differ significantly for these different refractive indices. We choose to parameterize the case of the refractive index 1.45+0.005i. Then it follows:

$$lg\langle Q_{\text{ext}}\rangle = \sum_{s=0}^{4} b_s lg^s x, \tag{8}$$

where $x=lg(2\pi a_{\text{ef}}/\lambda)$, $b_0=-0.367$, $b_1=1.76$, $b_2=-1.024$, $b_3=-0.095$ and $b_4=0.143$. The error of this approximation is small (see the solid line in Fig. 1).

The columnar aerosol concentration can be obtained from Eqs. (1) and (2) as

$$n = B\tau(\lambda_0), \tag{9}$$

where $B=\{\langle s\rangle\langle Q_{\text{ext}}(\lambda_0)\rangle\}^{-1}$. Therefore, n is directly related to the experimental measurement of the optical thickness at a given wavelength λ_0. In particular, it is advisable to use the wavelength λ_0 in UV for scenes over land, where the contribution of light reflected from the ground is low (von Hoyningen-Huene et al., 2003). Then generally unknown ground reflectance does not influence retrievals in a great extent.

The relationship (9) is often used in retrievals of the aerosol columnar concentrations from space (Griggs, 1975; Fraser et al., 1984; Kaufman and Fraser, 1990; Gasso and Hegg, 2003). The difference among various approaches is due to the different choice of the proportionality constant B, which is model-dependent. In the framework of our approach B is determined by just one factor and this is the effective radius of particles as specified above. We need to know a_{ef} to calculate the values of $\langle s\rangle$ and $\langle Q_{\text{ext}}\rangle$. The value of σ does not influence results considerably (at a_{ef}=const). So we choose for our parameterization: $\sigma \approx 0.8326$ as discussed above.

The effective radius can be estimated from the measured spectral optical thickness. Note that results of spectral measurements closely follow the following law:

$$\tau(\lambda) = \tau(\lambda_0)\left(\frac{\lambda}{\lambda_0}\right)^{-\alpha}, \tag{10}$$

where

$$\alpha = \frac{\ln\left\{\dfrac{\tau(\lambda)}{\tau(\lambda_0)}\right\}}{\ln\left\{\dfrac{\lambda_0}{\lambda}\right\}}. \tag{11}$$

The constant α is called the spectral exponent. It is easy to derive the value of spectral exponents from experimental measurements at two (or more) wavelengths. Also we can relate α to the size of particles calculating the dependence $\alpha(a_{\text{ef}})$ with Mie theory. The results of such calculations (but for the inverse function $a_{\text{ef}}(\alpha)$) at the refractive index 1.45+0.005i are shown in Fig. 2 by circles. The PSD used is the same as in Fig. 1. We find using the ORIGIN fitting procedure that the dependence a_{ef} (α) can be presented by the following formula valid at $a_{\text{ef}}\in[0.02\ \mu\text{m}, 0.7\ \mu\text{m}]$, which covers most of the variability range of a_{ef} for the atmospheric aerosol:

$$a_{\text{ef}} = p\exp(-u\alpha) + q\exp(-w\alpha), \tag{12}$$

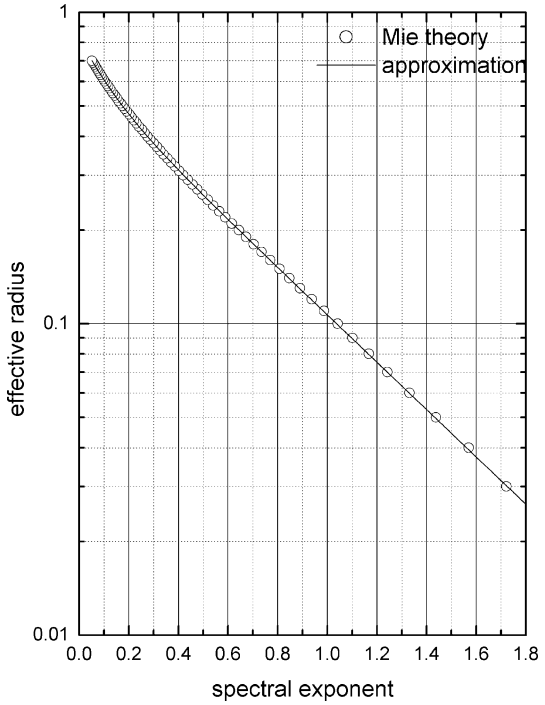

Fig. 2. Dependence of the spectral exponent on the effective size parameter calculated using Mie theory as indicated in the text.

where $p=0.61421$ μm, $u=1.750$, $q=0.217$ μm, $w=8.607$. Mie calculations of α (see Eq. (11)) have been done using wavelengths $\lambda_0=412$ nm and $\lambda=670$ nm. For back-of-envelope calculations, one can use: $a_{ef}=0.6\exp(-1.75\alpha)$. This equation clearly shows that the value of a_{ef} is smaller for larger α as one may expect from the physics of the problem.

Therefore, we conclude that both a_{ef} and n can be estimated using experimentally derived values of α and $\tau(\lambda_0)$ and also Eqs. (8), (9) and (12). The accuracy of retrievals depends on the proximity of the aerosol state during measurements to that used in the parameterization.

Although further studies of the accuracy of our approximation are needed, the derived parameterizations could provide potentially important insights in the spatial behavior of both the aerosol columnar concentration n and the size of scatterers a_{ef} as derived from space measurements. Also we can calculate the average aerosol columnar surface area $s=4n\langle s\rangle$ and the aerosol number concentration $N=n/L$, providing that the boundary layer height L is estimated from independent measurements. These parameters are of importance for atmospheric chemistry studies. The aerosol mass concentration M can be derived as $M=Nm_p$, where $m_p=\rho v_p$ is the average mass of an aerosol particle, ρ is the density of aerosol particles (e.g., 1.2 g cm^{-3}) and $v_p=a_m^3\exp(4.5\sigma^2)$ is the average volume of aerosol particles. Note that it follows approximately $v_p=\pi a_{ef}^3/6$ at $\Delta=1$. We can also introduce the columnar mass $m=ML$ and columnar volume $v=nv_p$.

Experimentally measured values of α and $\tau(\lambda_0)$ in combination with parameterizations discussed here can generate a number of atmospheric parameters important for the atmospheric

chemistry, climate modeling, and air quality studies (e.g., a_{ef}, M, m, N, n, s, v, and also $S=sL$, $V=vL$).

The next step is to assess the accuracy of our model. This will be a subject of a separate publication. The next section is devoted to the application of the derived relationships to satellite data in the vicinity of anthropogenic pollution sources.

3. Satellite aerosol retrievals

The Bremen Aerosol Retrieval Algorithm (BAER) (von Hoyningen-Huene et al., 2003) has been used to retrieve the parameters α and τ from SeaWiFs imagery of the Moscow region. Moscow is the largest industrial center of Russia with the population of approximately 11 000 000. Yet another 8 000 000 people live in a close vicinity to the city (so-called Moscow region). The city itself occupies 878.7 km^2. It is a largest pollution source in Europe. Therefore, it is of considerable importance to understand characteristics of both gaseous and particulate matter produced by the city together with its influence on the environment and human health.

One of the important indicators of the particulate matter over city is the aerosol optical thickness. The spatial distribution of the optical thickness at 412 nm as derived by BAER using SeaWiFs data registered at 10:57:44 UTC (around 2 p.m. Moscow local time, Tuesday) on September 7, 2004 is shown in Fig. 3. The spatial resolution of SeaWiFs is 1 km^2. It follows that the average aerosol optical thickness is close to 0.3 for most of the region except the central bow-type feature, where τ reaches 0.4 and even larger values. This feature is most probably best correlated with the Moscow traffic pattern.

The spatial distribution of the aerosol concentration as derived using parameterizations developed above in conjunction with the BAER-derived spectral exponent map is shown in

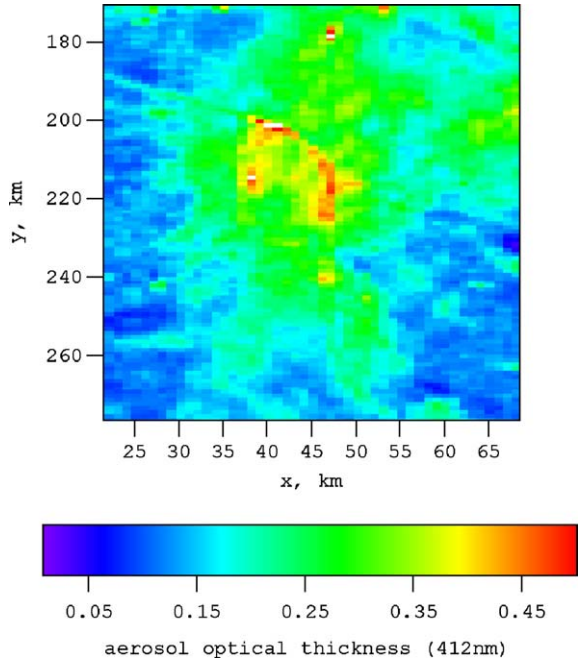

Fig. 3. The optical thickness map.

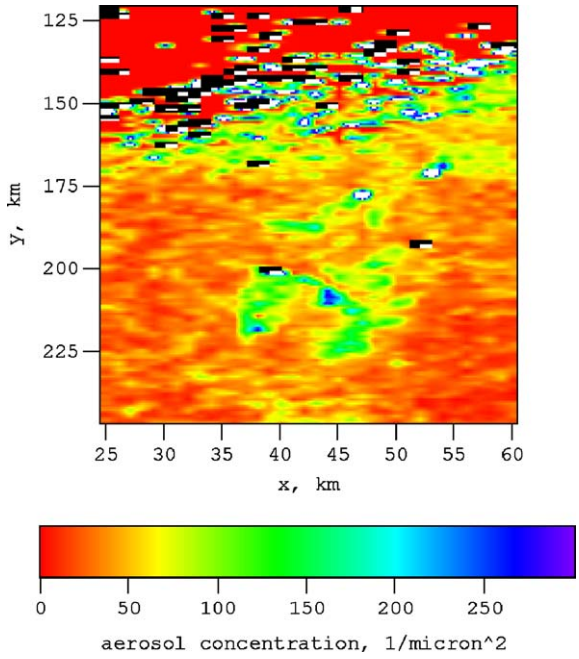

Fig. 4. The columnar number concentration map.

Fig. 4. It follows that $n \approx 100$ particles per squared micrometer. This is quite a huge load of particulate matter. Indeed assuming the boundary layer height $L=1$ km, we obtain the following estimation of the aerosol number concentration averaged over height $N=n/L \approx 10^5$ cm^{-3}. N is approximately 10 times smaller far away from the city center. There is a very non-uniform spatial distribution of n in the scene studied indicated a number of local pollution sources.

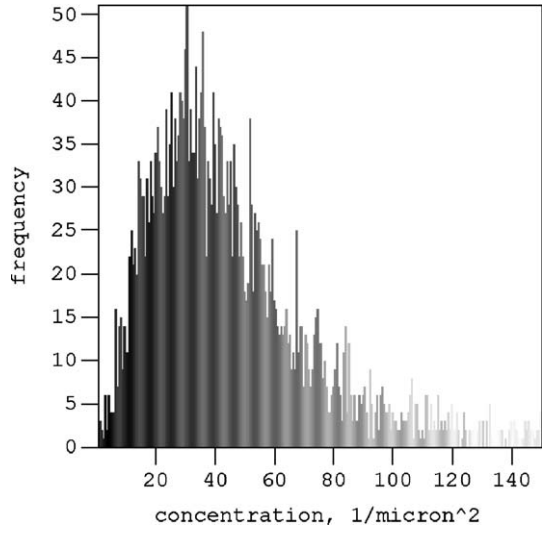

Fig. 5. Histogram of the columnar number concentration.

Table 1
Aerosol characteristics and their dimensions

Concentration	Symbol	Equation	Dimension	Assumptions
Mass concentration	M	$n\rho v_p/L$	1 μg m^{-3}	$L=1$ km, $\rho=1$ g cm^{-3}, $v_p=10^{-15}$ cm^3
Number concentration	N	n/L	1000 cm^{-3}	$L=1$ km

Data as shown in Figs. 5 and 6 are plotted for the aerosol columnar concentration n (in μm^{-2}). However, they remain unchanged for M and N, if dimensions as shown in the table are used under assumptions specified in the table ($n=1$ μm^{-2}). In particular, maximum of $n=30$ μm^{-2} in Fig. 5 corresponds to $M=30$ μg m^{-3} and $N=30\,000$ cm^{-3}, if assumptions as indicated in the table are fulfilled. The volume $v_p=10^{-15}$ cm^3 corresponds to a spherical particle having radius ≈ 0.062 μm.

The histogram shown in Fig. 5 suggests that $n \approx 30$ μm^{-2} on average for the scene studied and, therefore, $N \approx 30\,000$ cm^{-3} at $L=1$ km. We point out that n is proportional to M and N. Therefore, histogram as shown in Fig. 5 can be attributed also to values of M and N with dimensions shown in Table 1.

Such large values of N indicate quite a high mass load M. However, we need to know the distribution of the aerosol effective radius for the estimation of the aerosol mass. The map of a_{ef} as derived from satellite data using approach discussed in the previous section is shown in Fig. 6. Interestingly, the effective radius of particles appears to be smaller in the central part of the city indicating possibly enhanced gas-to-particle conversion processes in these areas. The histogram of the effective radius spatial distribution is shown in Fig. 7. It follows for the modal value of the effective radius: $a_{ef} \approx 0.1$ μm. This gives using equations presented in the previous section: $M \approx 20$ μg/m^3 as the average value with at least 5 times larger values in the central part of the city.

Note that Altshuller (1973) reported annual, arithmetic mean concentrations at urban sites in the range of 2.4–48.7 μg/m^3. This correlates well with our results. Also it is well known that the

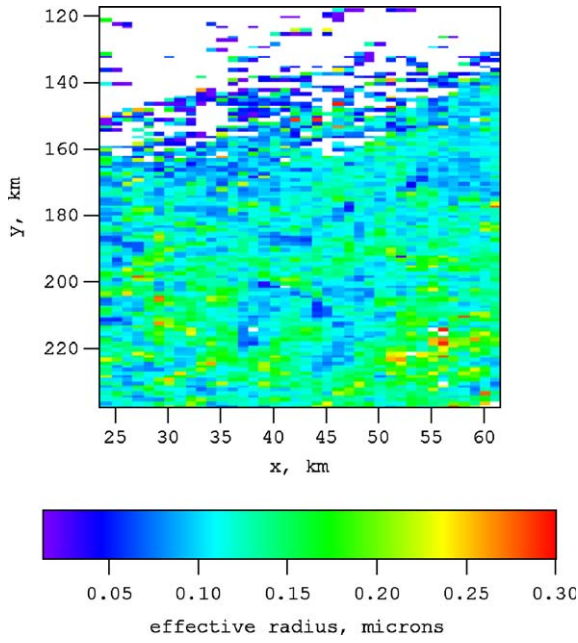

Fig. 6. The effective radius map.

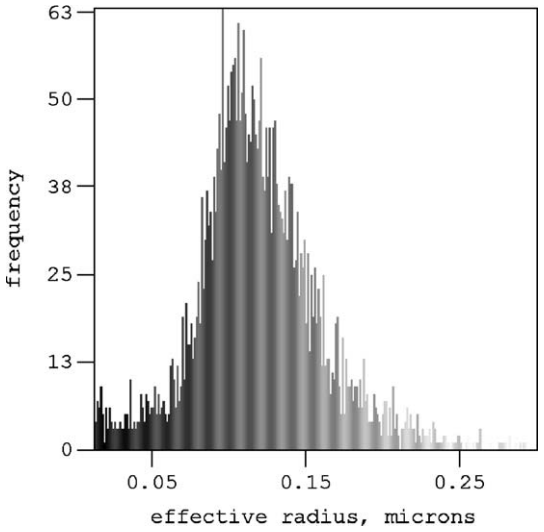

Fig. 7. Histogram of the effective radius.

concentration of pollutants in major cities can reach 100–200 μg/m^3. This is also confirmed by our study for the center of Moscow.

4. Conclusion

Summing up, we conclude that our parameterizations allow us to obtain reasonable values of atmospheric aerosol characteristics as derived from space measurements. Further studies involving ground-based measurements are needed to prove the technique and establish its accuracy. This, however, is not an easy task taking into account that ground-based measurements produce different results depending on the techniques used (e.g., filters, light scattering techniques, etc.). Also they are referred to the conditions at the ground level. Only average values of aerosol characteristics for the total atmospheric columns (or at least for the boundary layer) can be derived from satellite measurements. This information is relevant to climate studies. The aerosol microphysical characteristics measured by a satellite are also needed for global aerosol chemical models. They are relevant for human health studies in highly polluted environments.

We underline that further development of ideas presented in this paper may add an additional (satellite) dimension (see, e.g., Al-Saady et al., 2005) to standard air quality ground-based monitoring. This is of a special importance because our technique can be used as a basis for the automatic retrieval of the aerosol load at an arbitrary location.

Acknowledgements

This work has been supported by DFG Project BU 688/8-1.

References

Al-Saadi, J., et al., 2005. Improving national air quality forecasts with satellite aerosol observations. Bull. Am. Meteorol. Soc. 9, 1249–1261.

Altshuller, A.P., 1973. Atmospheric sulfur dioxide and sulfate: distribution of concentrations at urban and non-urban sites in the United States. Environ. Sci. Technol. 7, 709–712.

Fraser, R.S., 1976. Satellite measurement of mass of Sahara dust in the atmosphere. Appl. Opt. 15, 2471–2479.

Fraser, R.S., Kaufman, Y.J., Mahoney, R.L., 1984. Satellite measurements of aerosol mass and transport. Atmos. Environ. 18, 2577–2584.

Gasso, S., Hegg, D.A., 1997. Comparison of columnar aerosol optical properties measured by the MODIS airborne simulator with in situ measurements: a case study. Remote Sens. Environ. 66, 138–152.

Gasso, S., Hegg, D.A., 2003. On the retrieval of columnar aerosol mass and CCN concentration by MODIS. J. Geophys. Res. D108, doi:10.1029/2002JD002382.

Griggs, M., 1975. Measurements of atmospheric aerosols over water using ERTS-1 data. J. Air Pollut. Control Assoc. 25, 622–626.

Griggs, M., 1979. Satellite observations of atmospheric aerosols during the EOMET cruise. J. Atmos. Sci. 36, 695–698.

Kaufman, Y.J., Fraser, R.S., 1990. Satellite measurements of large-scale air pollution: methods. J. Geophys. Res. D95, 9895–9909.

King, M.D., Byrne, D.M., Herman, B.M., Reagan, J.A., 1978. Aerosol size distributions obtained by inversion of spectral depth measurements. J. Atmos. Sci. 35 (11), 2153–2166.

Kokhanovsky, A.A., von Hoyningen-Huene, W., Bovensmann, H., Burrows, J.P., 2004. The determination of the atmospheric optical thickness over Western Europe using SeaWiFS imagery. IEEE Trans. Geosci. Remote Sens. 42, 824–832.

Tanre, D., et al., 1999. Retrieval of aerosol optical thickness and size distribution over ocean from the MODIS airborne simulator during TARFOX. J. Geophys. Res. D104, 2261–2278.

von Hoyningen-Huene, W., Freitag, M., Burrows, J.P., 2003. Retrieval of aerosol optical thickness over land surfaces from top-of-atmosphere radiance. J. Geophys. Res. D108, doi:10.1029/2001JD002018.

Yamamoto, G., Tanaka, M., 1969. Determination of aerosol size distribution from spectral attenuation measurements. Appl. Opt. 8, 447–453.